Inorganic Chemistry

ARTICLE

pubs.acs.org/IC

Hydrolysis of Glycosides with Microgel Catalysts

Susanne Striegler,*[,†,‡] Michael Dittel,[‡] Rami Kanso,[†] Natasha A. Alonso,[†] and Evert C. Duin[†]

[†]Department of Chemistry and Biochemistry, 179 Chemistry Building, Auburn University, Auburn, Alabama 36849, United States

[‡]Division of Inorganic Chemistry II, University of Ulm, Albert-Einstein-Allee 11, 89069 Ulm, Germany

Supporting Information

ABSTRACT: A dormant macromolecular catalyst was prepared by polymerization of an aqueous styrene−butyl acrylate miniemulsion in the presence of a new polymerizable pentadentate ligand. The catalyst was activated by binding Cu(II) ions to the ligand site and then explored for its ability to hydrolyze glycosidic bonds in alkaline solution. The performance was correlated to the catalytic activity shown by low molecular weight analogs. A turnover rate of up to 43 × 10^{-4} min^{-1} was previously observed for cleavage of the glycosidic bond in selected *p*-nitrophenylglycosides with a binuclear, low molecular weight catalyst; by contrast, the same reaction is more than 1 order of magnitude faster and has a turnover rate of up to 380 × 10^{-4} min^{-1} when using the prepared macromolecular catalyst. The catalyzed hydrolysis is about 10^5-fold accelerated over the uncatalyzed background reaction under the provided conditions, while a significant discrimination of the α- and *β*-glycosidic bond or of the galacto- and gluco-configuration in the sugar moiety in the glycoside substrates is not observed.

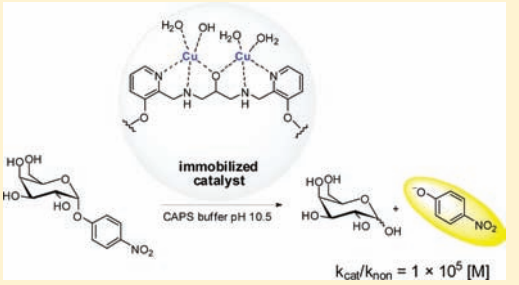

INTRODUCTION

Conventional multistep syntheses of oligosaccharides involve numerous protection and deprotection steps and obligatory activation of the glycosyl donors. While many elegant approaches for the syntheses of oligosaccharides have been developed,[1−14] they remain time consuming and most of them still require expert knowledge that limits automation. Selective catalytic transformations on carbohydrates remain particularly cumbersome, especially when underivatized sugar entities need to be transformed in aqueous solution, but corresponding enzymes are not known, are only available in limited quantity, are of insufficient purity, or possess a short shelf live. Catalytic entities promoting biomimetic reactions in the natural solvent of carbohydrates, i.e., water, would shorten time-consuming syntheses of oligosaccharides and open new directions beyond organic syntheses and medicinal chemistry by providing fast and convenient access to defined glycosides.

Our long-term goal in this context is preparation of macromolecular catalytic entities that allow selective in situ activation of underivatized glycosyl donors, thereby avoiding any lengthy activation or protection/deprotection steps of carbohydrates. This goal might be achieved by combining the catalytic transformation ability of transition metal complexes with the selectivity of a soluble templated polymer matrix. Previous results along these lines revealed that a macromolecular surrounding of a binuclear Cu(II) catalyst embedded in a water-soluble microgel matrix enhances its catalytic performance during oxidation reactions by about 1 order of magnitude compared to its low molecular weight analog.[15,16] Other preliminary data demonstrated the carbohydrate-discriminating ability of the binuclear

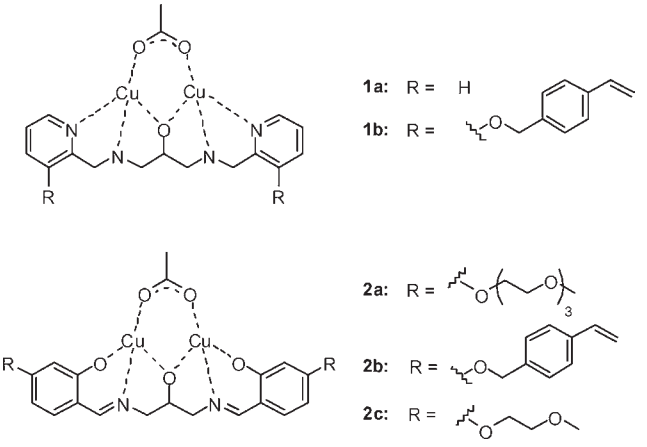

Figure 1. Structures of complexes **1a**,**b** and **2a**−**c**.

Cu(II) complex *N*,*N*′-{bis(2-pyridylmethyl)-1,3-diaminopropan-2-ol}ato dicopper(II) (*μ*-acetato) diperchlorate, Cu_2(bpdpo) (**1a**),[16−18] in alkaline solution (Figure 1); D-mannose is about 30-fold more tightly bound and recognized than D-glucose under comparable conditions.[18]

As a first step toward the long-term goal described above, we studied a variety of mono- and binuclear Cu(II) complexes as catalysts for hydrolysis of *p*-nitrophenylglycosides in aqueous solution.[19] Cleavage of the glycosidic bond was typically

Received: April 21, 2011
Published: August 15, 2011

Scheme 1. Synthesis of Pentadentate Backbone Ligand VB-(bsdpo) (3)

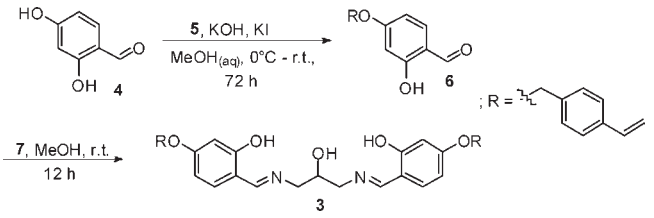

promoted more efficiently by bi- than by mononuclear Cu(II) complexes.[19] Complex **1a** was identified as the most proficient catalyst among those investigated as it accelerated hydrolysis of selected *p*-nitrophenylglycopyranosides up to 11 000-fold over the background reaction in CAPS buffer at pH 10.5 and 30 °C.[19] To some lesser extent, the reaction is also promoted by a binuclear copper(II) complex Cu_2(TEGbsdpo) (**2a**), which is derived in situ from *N*,*N*′-1,3-bis[{2-hydroxy-4-[2-(2-methoxyethoxy)ethoxy]ethoxy}benzylideneamino]propan-2-ol and copper(II) acetate (Figure 1).[19]

To enhance the catalytic turnover further, we and others hypothesized that a reagent immobilized in a polymer matrix might support selective interactions between a catalytic site and a substrate when constrained by the rigidity of a three-dimensional macromolecular matrix as observed in enzymes.[16] Corresponding synthetic entities might be assembled by arranging building blocks that enable hydrophobic interactions, $\pi-\pi$ stacking, and/or hydrogen bonding in addition to the coordinative bonds at a metal complex-containing active site in a cross-linked polymer matrix, such as a microgel. Immobilization of catalyst **1a** and **2a** in a polymeric environment lends itself as a promising strategy toward this goal. Along these lines, we herein report the synthesis and evaluation of macromolecular catalysts derived from polymerizable *p*-vinylbenzyl analogs of **1a** and **2a** (Figure 1).

RESULTS AND DISCUSSION

Synthesis of Pentadentate Backbone Ligands. As Cu(II) ions are paramagnetic limiting or even inhibiting radical polymerization reactions, the microgel catalysts are typically obtained by embedding the backbone ligands in a macromolecular matrix followed by coordination of Cu(II) ions to activate the dormant catalysts. Along these lines, a polymerizable ligand *N*,*N*′-1,3-bis[(2-hydroxy-4-vinylbenzyloxy)benzylideneamino]propan-2-ol, VBbsdpo (**3**), was prepared as reported recently (Scheme 1).[16,20,21] In short, commercially available 4-hydroxysalicylaldehyde (**4**) was treated with *p*-vinylbenzyl chloride (**5**) in the presence of a base and potassium iodide in a Williamson ether synthesis yielding (*p*-vinylbenzyloxy)salicylaldehyde (**6**).[16] Consecutive condensation of **6** with 1,3-diaminopropanol (**7**) afforded **3** in good yields and high purity after recrystallization from ethyl acetate. The yellow solid was stored without further precaution at ambient temperature prior to use for synthesis of the microgel catalysts.

The same synthetic strategy toward the preparation of 1,3-bis((3-(4-vinylbenzyloxy)pyridin-2-yl)methylamino)propan-2-ol, VB(bpdpo) (**8**), the backbone ligand of **1b**, failed, as attempts to derivatize 3-hydroxypyridinecarbaldehyde (**9**) in a Williamson ether synthesis gave no reaction product (Scheme 2).[22]

To overcome this limitation, a different synthetic strategy was developed by treating 2-(hydroxymethyl)pyridine-3-ol hydrochloride (**10**)[23] with **5** and base to afford (3-(4-vinylbenzyloxy)-pyridin-2-yl)methanol (**11**).[24] Swern oxidation conditions did not promote any apparent oxidation of **11** to 3-(4-vinylbenzyloxy)picolinaldehyde (**12**). Using commercially available manganese(IV) oxide in dimethoxyethane was futile as well, while freshly synthesized manganese(IV) oxide[25] in dimethoxyethane provided **12** in more than 91% yield after 8 h under reflux.[24] Likewise, selenium oxide in dry dioxane promotes oxidation of **11** into **12** nearly quantitatively in about 3 h.[26]

Isolation of aldehyde **12** was found to be cumbersome, leading to complete product loss due to polymerization upon standing in neat or diluted solutions at ambient temperature or in the cold under argon atmosphere or in the dark within 24 h. Consequently, only an analytical sample of aldehyde **12** was purified by flash column chromatography on silica gel using gradient elution with cyclohexane and ethyl acetate to allow full compound characterization. Attempts to purify **12** over basic aluminum oxide resulted in complete compound loss. As analysis of the raw material by ^{1}H and ^{13}C NMR spectroscopy indicated only minor amounts of impurities, aldehyde **12** was typically not further purified and used for immediate preparation of ligand **8**, as obtained from the reaction mixture after filtration and evaporation of the solvent.

Successful condensation of **12** with 1,3-diaminopropanol (**7**) yielding 1,3-bis((*E*)-(3-(4-vinylbenzyloxy)pyridin-2-yl)methyleneamino)-propan-2-ol (**13**) is indicated by ESI mass spectrometry (see Supporting Information). Subsequent reduction of the Schiff-base ligand **13** with sodium borohydride afforded **8** as a yellow-brownish oil after purification by size exclusion chromatography on Sephadex LH-20 with methanol as the eluent. Efforts to purify **8** by column chromatography over silica gel and neutral aluminum oxide resulted in compound decomposition; an analytical sample was purified by preparative-scale HPLC over RP-18 eluting with acetonitrile−water. Purified ligand **8** was stored neat in the dark at −18 °C prior to preparation of microgels or used immediately for preparation of binuclear Cu(II) complexes.

Preparation and Characterization of Polymerizable Binuclear Cu(II) Complexes: Synthesis of Cu_2(VBbsdpo). The binuclear Cu(II) complex *N*,*N*′-{1,3-bis[(2-hydroxy-4-(p-vinylbenzyloxy))-benzylideneamino]-propan-2-ol}ato dicopper (μ-acetate), Cu_2-(VBbsdpo) (**2b**), was derived from **3** after treatment with Cu(II) acetate in methanol as an amorphous powder; recrystallization of **3** in the same solvent and slow solvent evaporation yielded single crystals of **3** suitable for X-ray analysis.[16] The composition of **2b** in the solid state was confirmed by elemental analysis and mass spectrometry;[16] the coordination of the Cu(II) ions to the backbone ligand **3** was characterized by IR spectroscopy.[16] Single-crystal analysis of complex **2b** by X-ray diffraction revealed a square planar coordination environment for both Cu(II) ions, which are bridged by an endogenous μ-alkoxo oxygen atom of the backbone ligand **3** and an exogenous μ-1,3-coordinating acetate group providing N_1O_3 donor sets for both Cu(II) ions (Figure 2). Very similar bond lengths and angles are reported for binuclear Cu(II) complexes derived from Schiff-base ligands related to **2b**, which are obtained from other salicylaldehyde derivatives and **7**.[19,28] Discussion of the structural features of **2b** is consequently shortened herein. Selected bond lengths, bond angles, and torsion angles are listed in Table 1. The structure of Cu_2-(VBbsdpo) (**2b**) is confirmed as $Cu_2(3_{-3H})(OAc)$ in the solid state with an intermetallic Cu···Cu distance of 3.514(5) Å.[29]

dx.doi.org/10.1021/ic200837z |*Inorg. Chem.* 2011, 50, 8869–8878

Scheme 2. Synthesis of Pentadentate Backbone Ligand VB(bpdpo) (8)

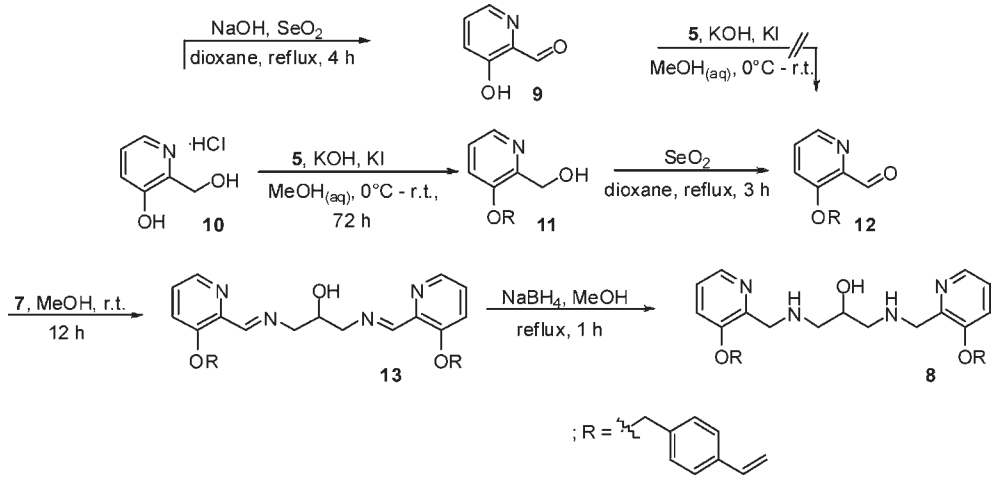

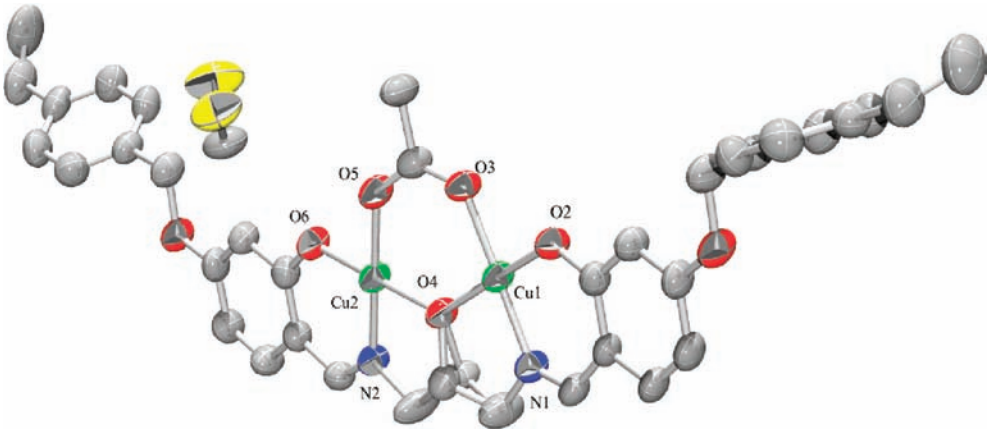

Figure 2. ORTEP[27]—POV ray representation for the structure of **2b**, Cu_2(VBbsdpo), depicted in ellipsoids with 70% probability; carbon atoms in gray, copper atoms in green, oxygen atoms in red, nitrogen atoms in blue, and chlorine atoms in yellow; all hydrogen atoms are omitted for clarity.

Table 1. Selected Bond Lengths [Å], Bond Angles [deg], and Dihedral Angles [deg] for Complex 2b, Cu_2(VBbsdpo)

bond lengths		bond angles		dihedral angles τ	
Cu(1)−O(2)	1.898(2)	O(2)−Cu(1)−O(4)	175.4(1)	O(2)−Cu(1)−O(4)−Cu(2)	103.4
Cu(1)−O(3)	1.955(2)	O(2)−Cu(1)−N(1)	94.2(1)	N(1)−Cu(1)−O(4)−Cu(2)	176.7
Cu(1)−O(4)	1.916(2)	O(4)−Cu(1)−N(1)	84.5(1)	O(6)−Cu(2)−O(4)−Cu(1)	111.1
Cu(1)−N(1)	1.919(2)	O(2)−Cu(1)−O(3)	87.4(1)	N(2)−Cu(2)−O(4)−Cu(1)	176.6
Cu(2)−O(4)	1.910(2)	O(4)−Cu(1)−O(3)	94.0(1)		
Cu(2)−O(5)	1.947(2)	N(1)−Cu(1)−O(3)	178.5(1)		
Cu(2)−O(6)	1.893(2)	O(6)−Cu(2)−O(4)	176.3(1)		
Cu(2)−N(2)	1.914(2)	O(6)−Cu(2)−N(2)	93.7(1)		
Cu(1)···Cu(2)	3.514(5)	O(4)−Cu(2)−N(2)	84.7(1)		
		O(6)−Cu(2)−O(5)	87.4(1)		
		O(4)−Cu(2)−O(5)	94.2(1)		
		N(2)−Cu(2)−O(5)	178.2(1)		
		Cu(1)−O(4)−Cu(2)	133.4(1)		

Similar intermetallic distances were previously noted for the two Cu(II) ions in {*N*,*N*′-1,3-bis[{2-hydroxy-4-(2-methoxyethoxy)}-benzylideneamino]propan-2-ol}ato (μ-acetato) dicopper complex Cu_2(EGbsdpo), **2c** (3.506(5) Å, Figure 1).[19] Thus,

dx.doi.org/10.1021/ic200837z |*Inorg. Chem.* 2011, 50, 8869–8878

derivatization of the ligand backbone structure of salen-type pentadentate ligands at their periphery does not influence the intermetallic distance in binuclear Cu(II) complexes derived thereof.

Preparation and Characterization of Polymerizable Binuclear Cu(II) complexes: Synthesis of Cu_2(VBbpdpo). The binuclear copper(II) complex *N*,*N*′-{bis((3-(4-vinylbenzyloxy)-2-pyridylmethyl)-1,3-diaminopropan-2-ol}ato dicopper(II) (μ-acetato) diperchlorate, Cu_2(VBbpdpo) (**1b**) was obtained from **8** by treatment with copper(II) acetate in the presence of sodium perchlorate in ethanol. The residue obtained after evaporation of the solvent was recrystallized from dichloromethane—methanol, yielding **1b** as a blue amorphous powder. ***Caution: perchlorate salts are potentially explosive. However, we did not experience any difficulty in handling or drying the compound below 40 °C.***

The composition of **1b** in the solid state was confirmed by elemental analysis. The coordination of the copper(II) ions to the backbone ligand **8** was indicated by IR spectroscopy. The N—H stretch vibrational band of the secondary amino groups in ligand **8** is shifted from 1631 to 1620 cm^{-1} after complexation with copper(II) ions in **1b**; likewise, the C═N stretch vibrational band of the pyridine groups changed from 1571 to 1577 cm^{-1} upon metal coordination (see Supporting Information). The aliphatic C—O stretching band found at 1116 cm^{-1} in **8** cannot be unambiguously assigned to a vibration in **1b** due to overlap with very strong perchlorate vibrational bands at 1092 cm^{-1}. Nevertheless, comparable assignments of the observed infrared vibrational bands were made previously for related ligands and their Cu(II) complexes.[19,30] Single crystals of **1b** suitable for X-ray diffraction were not obtained yet despite all efforts.

Synthesis and Purification of the Microgel Catalysts. Microgels derived from styrene (**14**), butyl acrylate (**15**), and Schiff-base ligand **3** were prepared by a protocol developed and described previously.[20] However, applying the elaborated procedure to the preparation of microgels from pentadentate ligand **8** led to visible phase separation in the polymerization mixture after about 1 h. Consequently, the amount of **8** was lowered to a nominal concentration of 1 mM for preparation of pol**8** and the amount of **3** for the preparation of pol**3** adjusted accordingly. In short, polymerization of the miniemulsion prepared from **14**, **15**, decane, and L (L = **3** or **8**) in 5 mM CAPS buffer at pH 10.5 containing sodium dodecyl sulfate was initiated by addition of potassium peroxysulfate solution to the preheated emulsion at 72 °C. Incorporation of pentadentate ligand **3** in pol**3** was previously shown to be nearly quantitative.[20] The same recipe was applied to prepare a control polymer in the absence of ligand, while the amount of DMSO solvent was kept constant.

All polymers pol**3**, pol**8**, and pol_{blank} were subsequently purified by dialysis in nanopure water and CAPS buffer for 24 h; the microgels pol**3** and pol**8** were then explored for their metal-ion binding ability prior to their use as catalysts. A detailed discussion of the physical characterization of microgel pol**3** is given elsewhere;[20] the morphology of pol**8** is a topic of ongoing investigation.

Activation of the Dormant Catalysts by Metal-Ion Loading. The previously observed insufficient binding of Cu(II) ions to pol**3** in nanopure water at pH 5.5 prompted a study of the metal binding ability of water-soluble TEGbsdpo (**3a**) as an analog of the polymerizable, water-insoluble ligand **3** (Chart 1).[20]

The spectrophotometric titration method developed by Zuberbühler et al. was used to determine complex formation

Chart 1. Structures of the Polymerizable Ligands 3 and 8 and Their Water-Soluble Analogs 3a and 8a

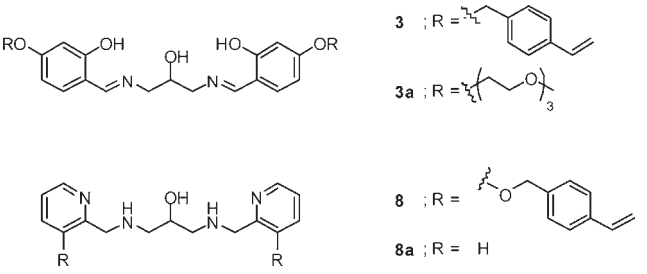

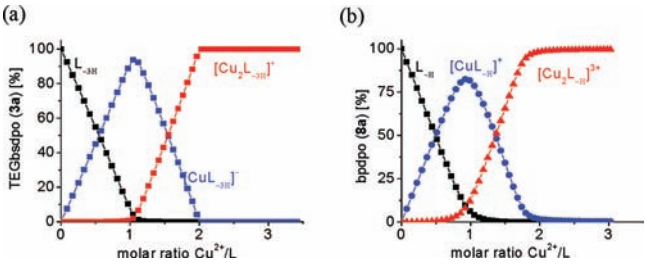

Figure 3. Complex formation upon titration of a solution of (a) 0.02 mM TEGbsdpo ligand (**3a**) and (b) 0.02 mM bpdpo ligand (**8a**) with 10 μL aliquots of a 0.30 mM aqueous Cu(II) acetate solution in 50 mM CAPS buffer at pH 10.5.

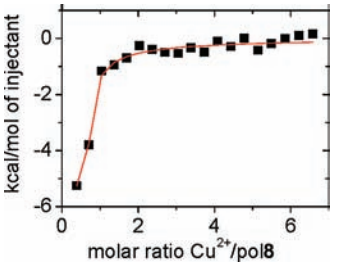

Figure 4. Titration of a 20 mM $Cu(OAc)_2$ solution into 0.1 mM pol**8** solution in 5 mM CAPS buffer at pH 10.5 and 30.0 ± 0.1 °C; $K_1 = 5.8 \times 10^6$, $\Delta H_1 = -7100 \pm 1200$ kcal/mol, $\Delta S_1 = 7.6$ cal mol^{-1} K^{-1}; $K_2 = 1.5 \times 10^7$, $\Delta H_2 = 1800 \pm 1200$ kcal/mol, $\Delta S_2 = 39.0$ cal mol^{-1} K^{-1}.

between TEGbsdpo (**3a**) and Cu(II) acetate dependent upon the pH of the solution.[31] A mononuclear $[CuL]^{2+}$ complex was determined as the major species at pH 5.5, and this explained the observed insufficient metal-ion binding ability of pol**3** under these conditions; binuclear species $[Cu_2L_{-2H}]^{2+}$ and $[Cu_2L_{-3H}]^{+}$ (L = TEGbsdpo) may, however, form in alkaline solution.[20] Previous studies with low molecular weight complexes furthermore revealed that catalytic hydrolysis of the glycosidic bonds in *p*-nitrophenylglycosides as model substrates requires a pH higher than 9.[19]

These previous results built the foundation for the herein described investigation of catalyst activation at pH 10.5 and subsequent study of their catalytic activity during cleavage of glycosidic bonds. Characterization of complex formation between ligands **3a** and **8a** and Cu(II) ions revealed the presence of mono- and binuclear copper(II) complexes, depending on the amount of metal ion, and ensured the absence of free metal ions.

dx.doi.org/10.1021/ic200837z |*Inorg. Chem.* 2011, 50, 8869–8878

Scheme 3. Putative Composition of 2a, Cu_2(TEGbsdpo), at pH 10.5

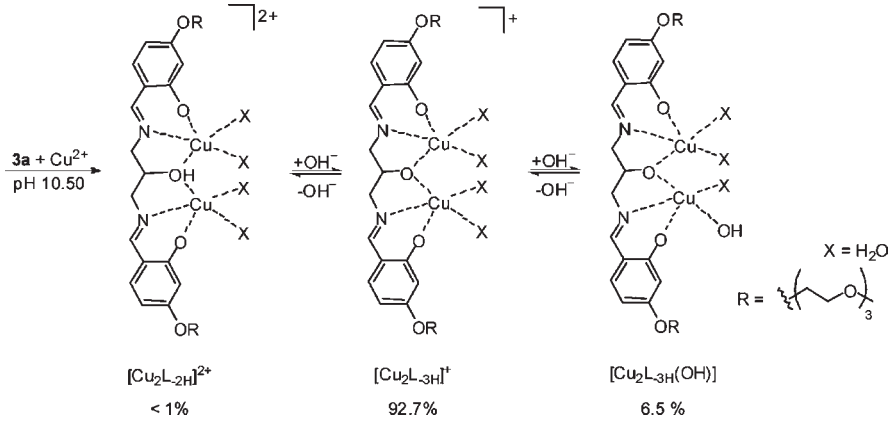

When titrating a solution of the TEGbsdpo ligand (**3a**) with aqueous Cu(II) acetate at pH 10.5, a mononuclear Cu(II) species $[CuL_{-2H}]$ (L = **3a**) forms initially and is successively replaced by a binuclear complex $[Cu_2L_{-3H}]^+$. The ligand is transformed into a binuclear Cu(II) species at a molar ratio of 2:1 between Cu(II) ions and **3a**. Hypothetical formation of a trinuclear species was included in the computation of the spectroscopic titration data but is not verified by the experimental data, even if the molar ratio between Cu(II) ions and the ligand exceeds 2:1 (Figure 3a). Comparable speciation data are obtained for the bpdpo ligand (**8a**) under identical conditions (Figure 3b).

To further characterize complex formation not only for small molecular weight analogs but more importantly for the polymers under investigation, we followed the titration of aqueous Cu(II) acetate solution into pol**8** by isothermal titration calorimetry (ITC) in CAPS buffer at pH 10.5 (Figure 4). The buffer concentration was lowered from 50 to 5 mM to reduce the large background noise; data are corrected for unspecific binding of Cu(II) ions to a control polymer that does not contain a ligand. The best fit of the ITC data was provided by a sequential binding model indicating a molar ratio of 2:1 for coordination of the metal ions to the ligand binding site in pol**8**. The titration data indicate coordination of two metal ions, supporting the results obtained from the speciation data (vide infra). For the following kinetic and electron spin resonance (EPR) experiments, appropriate amounts of aqueous Cu(II) acetate solutions were added to the dialyzed microgels pol**3** and pol**8** to activate the catalysts polCu_2**3** and polCu_2**8** in CAPS buffer at pH 10.5; the nominal catalyst concentration is 0.1 mM.

Characterization of the Complex Composition at pH 10.5. To probe for possible structural changes around the Cu(II) ions caused by immobilization of the backbone ligand, the low molecular weight complexes and their microgel analogs were evaluated by EPR spectroscopy. The spectra observed for the activated microgels polCu_2**8** and polCu_2**3** are correlated to those of their corresponding small molecular weight entities **1a** and **2a**. All spectra were recorded at 77 K and corrected for background signals by subtraction of the buffer spectrum. The composition of the low molecular weight entities at pH 10.5 is known from spectrophotometric titration experiments conducted previously.[18,19,32]

In brief, the in situ prepared complex **2a** exists in about 93% as binuclear $[Cu_2L_{-3H}]^+$ (L = **3a**) species coordinating water molecules to the metal-ion core and less than 7% exist as a $[Cu_2L_{-3H}(OH)]$ species (Scheme 3). By contrast, a $[Cu_2L_{-H}(OH)]^{2+}$ species is predominant (L = **8a**) when dissolving complex **1a** at pH 10.5, while about 11% of the complex is forming a $[Cu_2L_{-H}(OH)_2]^+$ species (Scheme 4).[18] Previous studies revealed that the acetate anion coordinated to the metal core in **1a** in the solid state is preserved in methanol[32] but not in aqueous organic solution.[33]

The Cu signal in the EPR spectra of all samples is insignificant with an insufficient signal to noise ratio when imitating the conditions used during catalysis due to the low nominal complex concentration in the microgels (0.01 mM, see below). However, concentration-dependent studies with complex **1a** indicate that sufficient Cu signal is observable for concentrations between 0.05 and 1 mM (data not shown). Due to practical limitations caused by dialysis of the microgels and subsequent catalyst activation, a nominal metal complex concentration of 0.05 mM was used for all EPR experiments thereafter. On average, 80% of the Cu signal is detectable as determined by spin quantization under nonsaturating conditions.

The electronic environment around the Cu ions in the low molecular weight complexes **1a** and **2a** is different due to the H-bond-donating and H-bond-accepting nature of the backbone ligands (Chart 1). Consequently, different EPR spectra for complexes **1a** and **2a** (Figure 5) are observed. However, the EPR spectra of complex **1a** and its corresponding microgel polCu_2**8** are alike, indicating that the complex does not undergo large structural changes due to immobilization in a microgel. Slight line broadening reflecting restricted orientation of the immobilized catalyst is noted for the microgel polCu_2**8** in comparison to **1a**. Complex **2a** and microgel polCu_2**3** behave likewise.

The results of the EPR experiments suggest that the catalytically active species in the microgels is very similar to those of the low molecular weight complexes and does not provide a rational for the dramatically increased catalytic activity observed by the microgels (see below). Further experiments in this regard and modifications of the microgels to increase the catalyst loading are topics of ongoing investigations.

Evaluation of pol$Cu_2$3 and pol$Cu_2$8 as Catalysts for Cleavage of Glycosidic Bonds. In order to evaluate the ability of the macromolecular entities to hydrolyze glycosidic bonds in comparison to their small molecular weight analogs, catalytic hydrolysis of *p*-nitrophenyl-α-D-galactopyranoside (**16**) into galactose and *p*-nitrophenolate was followed using UV−vis spectroscopy (Scheme 5).[19] The reaction was previously shown to depend

dx.doi.org/10.1021/ic200837z |*Inorg. Chem.* 2011, 50, 8869–8878

Scheme 4. Putative Composition of 1a, Cu_2(bpdpo), at pH 10.5

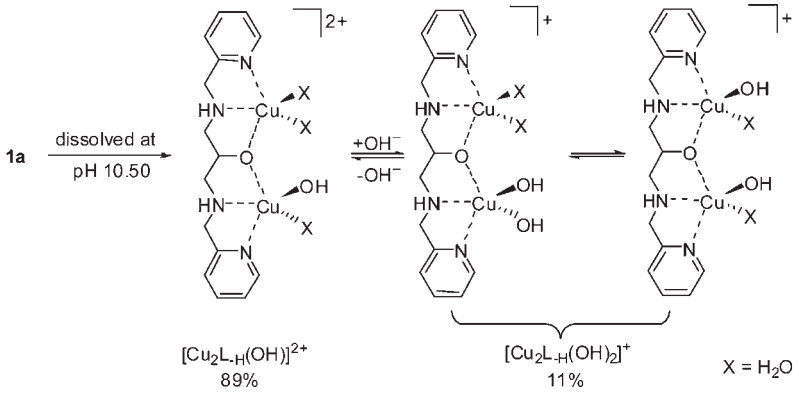

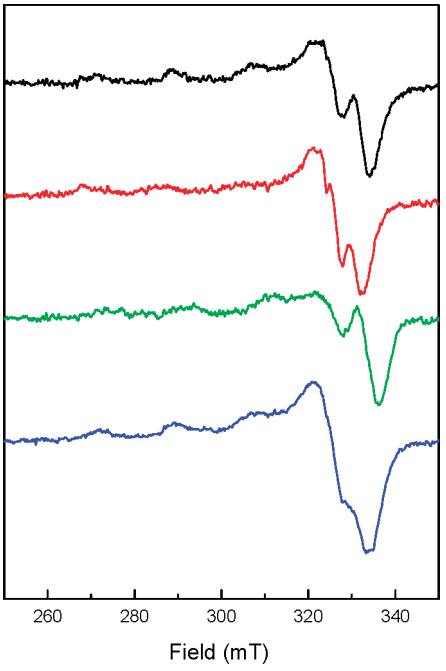

Figure 5. EPR spectra of complexes Cu_2(bpdpo) (**1a**, black line) and Cu_2(bsdpo) (**2a**, green line) and of the corresponding activated microgels polCu_2**8** (red line) and polCu_2**3** (blue line) at 77 K.

linearly on the catalyst concentration, to require a pH above 9, and to proceed with higher efficiency for the binuclear complex **1a** in comparison to **2a** or mononuclear analogs thereof (Figure 1).[19] Attempts to increase the substrate concentration to reach saturation of the catalytic sites are limited by the solubility of the selected substrates **16**, *p*-nitrophenyl-β-D-galactopyranoside (**17**), *p*-nitrophenyl-α-D-glucopyranoside (**18**), and *p*-nitrophenyl-β-D-glucopyranoside (**19**).[19] Nevertheless, pseudo-first-order conditions were provided with excess of substrate in concentrations between 5 and 35 mM (Table 2).

The turnover rate for hydrolysis of **16** in the presence of metal-free polymers pol**3** and pol**8** is on the same order of magnitude as its free hydrolysis in solution ($k_{non} = 3.8 \times 10^{-7}$ min^{-1}; $k_{non,pol3} = 5.2 \times 10^{-7}$ min^{-1}; $k_{non,pol8} = 3.4 \times 10^{-7}$ min^{-1}). Hydrolysis of the substrates is not promoted by a Cu(II) acetate solution, as precipitation of Cu(II) hydroxide is observed at pH 10.5 instead.

The low molecular weight catalysts **1a** and **2a** were previously found to cleave the glycosidic bond in substrate **16** with a catalytic turnover of up to 43×10^{-4} min^{-1}, a moderate efficiency (k_{cat}/K_M), and an acceleration (k_{cat}/k_{non}) of the hydrolysis of up to 11 000-fold over the background reaction (Table 2, entries 1 and 2).[19] By contrast, the macromolecular catalyst polCu_2**3** increases the catalytic efficiency for hydrolysis of the glycosidic bond in **16** by about an order of magnitude in comparison to **2a** (Table 2, entries 2 and 3); use of macromolecular polCu_2**8** instead of small molecular weight complex **1a** increases the catalytic efficiency even further (Table 2, entries 1 and 4). Acceleration of the reaction and the catalytic efficiency of the hydrolysis of substrates **17**−**19** by polCu_2**8** is also comparable to hydrolysis of **16**, accounting for a high catalytic activity of the macromolecular catalyst toward cleavage of glycosidic bonds (Table 2, entries 5−7); however, catalyst polCu_2**8** is not capable of differentiating α- or β-glycosidic linkages or the gluco or galacto configuration of the sugar substrates. Nevertheless, the results are remarkable as the catalytic proficiency ($k_{cat}/(K_m k_{non})$) of polymer polCu_2**8** toward the investigated substrates is as high as 5.6×10^7 in alkaline solution and thus more than 3 orders of magnitude higher than the proficiency determined for its small molecular weight analog **1a**. Stimulated by these encouraging results, current studies are directed toward templating the catalyst polCu_2**8** to enable a selective cleavage of glycosidic bonds with macromolecular catalysts in the near future.

SUMMARY OF RESULTS

Macromolecular entities were prepared and explored as catalysts to enhance the hydrolysis of glycosidic bonds in comparison to small molecular weight analogs. Along these lines, pentadentate ligand **3** was synthesized as previously disclosed, while a feasible synthesis for the new polymerizable pentadentate ligand VB(bpdpo) (**8**) was developed and described herein. Binuclear copper(II) complexes Cu_2(VBbpdpo), **1b**, and Cu_2(VBbsdpo), **2b**, were subsequently derived from VB(bpdpo), **8**, and VB(bsdpo), **3**, respectively, and characterized in the solid state. Analysis of single crystals of **2b** suitable for X-ray diffraction revealed that derivatization of the backbone ligand at its periphery does not alter the geometry of the donor atoms around the metal ion core nor the metal−metal ion distance in the binuclear complex.

Polymers prepared from aqueous miniemulsions of styrene or butyl acrylate in the presence of **3** or **8**, respectively, lead to

dx.doi.org/10.1021/ic200837z |*Inorg. Chem.* 2011, 50, 8869–8878

dormant catalysts. The nominal ligand concentration should not exceed 1 mM to avoid phase separation during polymerization. The dormant catalysts can be activated by coordination of Cu(II) ions; sufficient metal-ion loading ability between Cu(II) ions and the backbone ligand in a 2:1 molar ratio was observed and followed by isothermal titration calorimetry. The results are in agreement with the Cu(II)-ion binding ability determined for small molecular weight analogs by spectrophotometric titration.

Glycosidic hydrolysis of *p*-nitrophenylglycoside model substrates in alkaline aqueous solution was previously observed with a turnover rate of up to 43×10^{-4} min^{-1} for **1a**; the same reaction is more than 1 order of magnitude faster and has a turnover rate of up to 380×10^{-4} min^{-1} when using the macromolecular catalyst polCu$_2$**8** under otherwise identical conditions. The reaction is about 10^5-fold accelerated over the uncatalyzed background reaction. A similar enhancement was previously observed for acceleration of catalytic oxidation of derivatized catechols into quinones by macromolecular catalysts.[16] However, the polCu$_2$**8** catalyst does not discriminate between α- or β-glycosidic linkages or the gluco and galacto configurations of the carbohydrate moieties of the selected substrates. Current efforts are therefore directed toward templating the matrix during material preparation to provide microgel catalysts with sufficient selectivity during hydrolysis of glycosidic bonds in the near future.

EXPERIMENTAL SECTION

Instrumentation. ^{1}H and ^{13}C NMR spectra were recorded on a Bruker AV400 (400.2 MHz for ^{1}H and 100.6 MHz for ^{13}C). Chemical shifts (δ) in ^{1}H NMR spectra are expressed in ppm and coupling constants (J) in Hertz. Signal multiplicities are denoted as s (singlet), d (doublet), t (triplet), q (quartet), and m (multiplet). Deuterated chloroform and DMSO-d_6 were used as solvents, and chemical shift values are reported in ppm relative to the residual signals of these solvents ($CDCl_3$ δ = 7.29 for ^{1}H and δ = 77.0 for ^{13}C; DMSO δ = 2.59 for ^{1}H and δ = 39.5 for ^{13}C). MS analysis of samples was performed using an Ultra Performance LC Systems (ACQUITY, Waters Corp., Milford, MA) coupled with a quadrupole time-of-flight mass spectrometer (Q-TOF Premier, Waters) with electrospray ionization (ESI) in both ESI-MS and ESI-MS/MS modes operated by the Masslynx software (V4.1). X-ray analysis was performed on a Bruker SMART APEX CCD X-ray diffractometer. IR spectra of oils were recorded as thin films on KBr discs; solids were measured as KBr pellets with a resolution of 0.5 cm^{-1} using a Shimadzu IR Prestige-21 FT-Infrared Spectrometer; ν in cm^{-1}. UV−vis spectra were recorded at 30.0 ± 0.1 °C over a range of 200−800 nm on a Varian Cary 50 with WinUV Analysis Suite software, version 3.0, using disposable Brandtech macrocells (220−900 nm) of 1 cm thickness and 4.5 mL volume for determination of the distribution of species. Disposable 1.5 mL semimicro Brandtech UV cuvettes (220−900 nm) of 10 mm light path with caps were used for the hydrolysis studies. Isothermal titration calorimetry (ITC) was performed on a VP isothermal titration calorimeter (Microcal Inc., Northampton, MA) at 300 K; the reference cell was loaded with nanopure water. EPR spectra were obtained with a Bruker EMX spectrometer at X-band (9383 MHz) and fitted with the ER-4119-HS perpendicular-mode cavity. Sonication was performed with a Digital Sonifier from Branson equipped with a disruptor horn and a tapered 1/8 in. microtip at a 70% amplitude for 2 min. Samples for elemental analysis were sent to Atlantic Microlab Inc., Atlanta, GA, or obtained on the CHN-O-RAPID instrumentation (Heraeus), Ulm University, Germany. The pH values were measured using a Beckman Φ 250 pH meter equipped with a refillable long Futura pH electrode of 0.7 mm thickness. The pH meter was calibrated before each set of readings (3-point calibration). All melting points were recorded on a Mel-Temp melting point apparatus, and the values are uncorrected. Thin layer chromatography (TLC) was performed using silica gel TLC plates from SORBENT Technologies, 200 μm, 4 × 8 cm, aluminum backed, with fluorescence indicator F_{254} and detection by UV light or charring with an aqueous vanillin−sulfuric acid reagent and subsequent heating of the TLC plate. Column chromatography was carried out using silica gel 60 from Silicycle (40−63 μm, 230−240 mesh) or basic aluminum oxide (pH range 9.7 ± 0.4, activity I), 32−63 μm, surface area 150 m^2 g^{-1} from Sorbent Technologies as stationary phase. Sephadex LH-20−100 was obtained from Fluka and equilibrated in methanol for 24 h prior to use. Nanopure water was obtained from an EASYpure II water system from Barnstead (18.2 MΩ/ cm). The dialysis membrane Spectra/Por Biotech (16 × 10 mm; 0.79 mL/cm; volume/length) had a molecular cutoff of 15 000 and was obtained from Spectrumlabs.

Scheme 5. Catalytic Hydrolysis of *p*-Nitrophenyl-α-D-galactopyranoside (16)

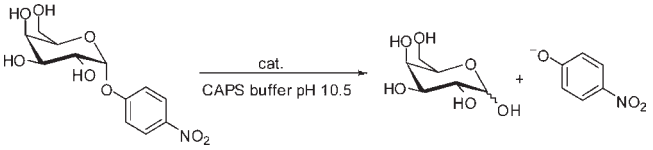

Table 2. Summary of Kinetic Parameters for the Catalytic Hydrolysis of *p*-Nitrophenyl-α/β-D-glycopyranosides in 50 mM CAPS buffer at pH 10.5 and 30 ± 0.1 °C[a]

entry	catalyst	S [M]	k_{cat} (× 10^{-4}) [min^{-1}]	K_M [mM]	k_{cat}/K_M [M^{-1} min^{-1}]	k_{cat}/k_{non} [M]	$k_{cat}/(K_m k_{non})$ (× 10^3)
				metal complexes[b]			
1[b]	**1a**	**16**	43 ± 10	210 ± 57	0.02	11 000	54
2[b]	**2a**	**16**	13 ± 3	150 ± 43	0.009	3300	22
				activated macromolecular catalysts			
3	polCu$_2$**3**	**16**	20 ± 1	20 ± 4	0.1	3800	192
4	polCu$_2$**8**	**16**	350 ± 60	2.7 ± 0.1	13	104 000	39 000
5		**17**	360 ± 44	1.9 ± 0.6	19	106 000	56 000
6		**18**	380 ± 20	4.6 ± 0.2	8	112 000	24 000
7		**19**	375 ± 10	3.0 ± 1.4	13	110 000	37 000

[a] k_{non} = 3.8 × 10^{-7} min^{-1}; $k_{non,pol3}$ = 5.2 × 10^{-7} min^{-1}; $k_{non,pol8}$ = 3.4 × 10^{-7} min^{-1}; ε_{sol} (*p*-nitrophenolate, 400 nm) = 16 190 M^{-1} cm^{-1}; ε_{pol} (*p*-nitrophenolate, 400 nm) = 24 400 M^{-1} cm^{-1}. [b] Data taken from ref 19.

dx.doi.org/10.1021/ic200837z |*Inorg. Chem.* 2011, 50, 8869–8878

Chemicals. The polymerizable ligand *N*,*N*′-1,3-bis[(2-hydroxy-4-vinylbenzyloxy)benzylideneamino]propan-2-ol, VBbsdpo (**3**),[16] its water-soluble analog *N*,*N*′-1,3-bis[{2-hydroxy-4-[2-(2-methoxyethoxy)-ethoxy]ethoxy}benzylideneamino]-propan-2-ol, TEGbsdpo (**3a**),[33] the {*N*,*N*′-1,3-bis[2-hydroxy-4-(vinylbenzyloxy)benzylideneamino]-propan-2-ol}ato (*μ*-acetato) dicopper complex, Cu_2(VBbsdpo) (**2b**),[16] {*N*,*N*′-1,3-bis[{2-hydroxy-4-[2-(2-methoxyethoxy)ethoxy]ethoxy}benzylideneamino]-propan-2-ol}ato (*μ*-acetato) dicopper complex, Cu_2-(TEGbsdpo) (**2a**), binuclear Cu(II) complex *N*,*N*′-{bis(2-pyridylmethyl)-1,3-diaminopropan-2-ol}ato dicopper(II) (*μ*-acetato) diperchlorate, Cu_2(bpdpo) (**1a**),[16−18] and 2-(hydroxymethyl)pyridine-3-ol hydrochloride **10**[23] were synthesized as described. Styrene (**14**) and butyl acrylate (**15**) were distilled under vacuum and stored under argon in the dark at 10 °C prior to use. All other chemicals were used as received from commercial suppliers.

Miniemulsion Polymerization: Typical Procedure. The poly(acrylate−styrene)−ligand microgels, polL (L = **3** or **8**), were prepared by mixing 0.30 g (2.3 mmol) of butyl acrylate, 0.30 g (2.9 mmol) of styrene, and 50 mg of decane with 4.8 mL of water containing 14 mg (0.05 mmol) of sodium dodecyl sulfate (SDS). The ligand (L = **3** or **8**, 5 *μ*mol) was dissolved in 50 *μ*L of DMSO and added to the monomer solution. The resulting mixture was cooled in ice, sonicated at 70% amplitude for 2 min, and heated to 72 °C under continued stirring. Polymerization was initiated after 10 min by addition of 0.4 mL of aqueous potassium peroxysulfate (20 mg, 0.07 mmol) solution and allowed to proceed for 90 min.

Polymer Purification by Dialysis. Dialysis membranes with a molecular weight cutoff of 15 kDa and a nominal diameter of 10 mm were soaked in Nanopure water for 30 min prior to immediate use and filled with 1 mL sample aliquots of the microgel stock solution. The tubing was subsequently closed and dialyzed against nanopure water for 2 h and four times for 6 h each against 5 mM CAPS buffer at pH 10.5 subsequently. The samples of the purified polymers were then diluted to 10 mL with the same buffer. The nominal concentration of the ligand in the resulting polymers was 0.1 mM. The control polymer pol_{blank} was treated identically.

Speciation Experiments. In a typical experiment, 2 mL of a 50 mM CAPS buffer solution at pH 10.5 that is 0.02 mM regarding the ligand (**3a** or **8a**) and 1.0 mM regarding the $NaClO_4$ concentration were titrated with 10 *μ*L aliquots of an aqueous 0.30 mM Cu(II) acetate solution at 30.0 ± 0.1 °C. UV−vis spectra were taken after each addition of an aliquot of the Cu(II) solution, and the resulting data were computed by the global fitting model provided by the program SpecFit.[31]

EPR Experiments: Typical Procedure. Complex **1a** (1.31 mg, 0.002 mmol) was dissolved in 2.0 mL of 50 mM CAPS buffer at pH 10.5 yielding a 1.0 mM stock solution; aliquots of this solution were further diluted to obtain samples with concentrations in the range of 0.01−1 mM and an overall sample volume of 300 *μ*L. Alternatively, a 0.05 mM sample was prepared by dissolving 1.64 mg (0.003 mmol) of complex **1a** into 50.0 mL of 50 mM CAPS buffer at pH 10.5.

Complex **2a** was prepared in situ as 0.05 mM solution from 20 *μ*L of a solution containing ligand **8a** (2.34 mg, 0.004 mmol) in 5.0 mL of 50 mM CAPS buffer at pH 10.5 and 20 *μ*L of a solution of copper acetate monohydrate (1.50 mg, 0.008 mmol) in 5.0 mL of nanopure water; the total volume of the sample was increased to about 300 *μ*L by addition of 260 *μ*L of buffer, yielding the indicated concentration.

The microgels polCu_2**8** and polCu_2**3** were prepared and dialyzed as described, yielding solutions with a nominal concentration of 0.1 mM with respect to the metal complex in 5 mM CAPS buffer. Samples for EPR measurements were prepared by diluting 150 *μ*L of the dialyzed microgel solutions with 150 *μ*L of 50 mM CAPS buffer.

All spectra were recorded with a field modulation frequency of 100 kHz, the microwave power was 2 mW, and cooling of the samples was performed with a liquid-nitrogen finger Dewar (77 K). Spin quantization was carried out under nonsaturating conditions using an aqueous copper perchlorate solution as the standard (10 mM $CuSO_4$; 2 mM $NaClO_4$; 10 mM $HCl_{(aq)}$).

Isothermal Titration Experiments: Typical Procedure. An aliquot of the dialyzed polymer pol**3**, pol**8**, or pol_{blank} with a nominal ligand concentration of 0.1 mM in 5 mM CAPS buffer at pH 10.5 was placed in the sample cell. The reference cell was loaded with nanopure water. The polymers were subsequently titrated with 10 *μ*L aliquots of a 20 mM aqueous Cu(II) acetate solution at 30.0 ± 0.1 °C. The obtained data were fitted by the sequential binding site model implemented in the data collecting software Origin 7.0.

Catalytic Hydrolysis of Glycosides: Typical Procedure. In a typical experiment, the concentration of *p*-nitrophenylglycosides was 5−30 mM with a catalyst concentration of 0.01 mM in a solution with a total volume of 1.0 mL. All solutions were prepared or diluted into 50 mM CAPS buffer at pH 10.5. The substrate aliquots were diluted with buffer to a total volume of 900 *μ*L and equilibrated at 30 °C for 30 min. The reaction was initiated by addition of a 100 *μ*L aliquot of the equilibrated 0.1 mM catalyst solution. The proceedings of the reaction were monitored over time by recording the formation of the *p*-nitrophenolate using UV−vis spectroscopy at 400 nm. The background reaction was observed in a similar manner in the absence of a polymer catalyst or, alternatively, in the presence of the control polymer pol_{blank}. The extinction coefficient for product formation in the presence (ε_{sol}) and absence (ε_{sol}) of the microgel catalyst was determined by a calibration curve and used to convert the absorbance of the reaction product into molar amounts (*p*-nitrophenolate: ε_{sol} = 16 190 M^{-1} cm^{-1} and ε_{pol} = 24 400 M^{-1} cm^{-1}). The value for the extinction coefficients varies due to the turbidity in the solution caused by addition of the microgel catalysts.

(3-(4-Vinylbenzyloxy)pyridin-2-yl)methanol (11). Synthesis of **11** was achieved by modifying a procedure for preparation of 2-hydroxymethyl-3-benzyloxypyridine disclosed by Sheehan et al.[34] In short, an aqueous solution (50 mL) of potassium hydroxide (8.1 g, 0.14 mol) and potassium iodide (0.16 g, 1.0 mmol) was added to a solution of **10** in 50 mL of water. *p*-Vinylbenzylchloride (12 mL, 75 mmol) in 200 mL of methanol was then added dropwise while cooling the solution in an ice bath. Subsequently, methanol was added until the solution turned clear (∼150 mL), and stirring was continued for 72 h. The solution was concentrated after filtration in vacuum below 30 °C until phase separation occurred. The flask was kept at 8 °C for 24 h, during which time the darker orange layer solidified. A light yellow, microcrystalline product was separated by filtration and washed with ice-chilled methanol yielding 4.0 g (54%) of **11**; mp 95−96 °C; δ_H ($CDCl_3$) 8.19 (m, 1H, $-C_5H_3N$), 7.46 (dd, 2H, 7.3, 1.0, $-C_6H_4-$), 7.38, (dd, 2H, 7.3, 1.0, $-C_6H_4-$), 7.19 (d, 2H, 3.0, $-C_5H_3N$), 6.75 (dd, 1H, 17.7, 10.7, CH_2═C*H*), 5.80 (dd, 1H, 17.7, 0.8, C*H*$_2$═CH), 5.31 (dd, 1H, 10.5, 0.4, C*H*$_2$═CH), 5.13 (s, 2H, C*H*$_2-C_6H_4-$), 4.84 (s, 2H, $-CH_2-C_5H_3N$); 3.38 (bs, 2H, NH); δ_C 151.3, 148.7, 139.7; 137.6, 136.2, 135.4, 127.3, 126.5, 122.6, 117.9, 114.4, 69.7, 60.1. *ν* (KBr): 3433 (NH), 3075, 3023 (arom. CH), 2929, 2868 (aliph. CH), 1573 (C−N), 1445, 1408 (arom. C−C), 1276 (OH), 1054 (C−O) cm^{-1}. Anal. Calcd for $C_{15}H_{15}NO_2$: C, 74.67; H, 6.27; N, 5.81. Found: C, 74.63; H, 6.24; N, 5.71; HRMS, ESI-TOF (+), calcd for $C_{15}H_{16}NO_2$ $(M + H)^+$: 242.1881. Found: 242.1886.

3-(4-Vinylbenzyloxy)picolinaldehyde (12). Selenium dioxide (460 mg, 4.15 mmol) was added to a solution of **11** (1.0 g, 4.2 mmol) in 10 mL of dry 1,4-dioxane under argon at room temperature. The resulting suspension was stirred under reflux for 3 h and filtered through glass wool after cooling. The filtrate was concentrated under reduced pressure at 32 °C to yield **12** as an orange oil that was typically not further purified. For a full characterization of **12**, however, a sample aliquot of the residue was purified by flash chromatography over silica gel, eluting with a gradient of cyclohexane/EtOAc (2/1 to 1/1, v/v), yielding **12** as a colorless solid (TLC, SiO_2, cyclohexane/EtOAc, 1/1,

v/v, R_f = 0.6). A large loss of product was observed during purification due to putative polymerization to a gummy solid particularly during concentration of any solution containing **12** prior to and after gel chromatography. Use of aluminum oxide instead of silica gel resulted in complete product loss and was for that reason not pursued further; mp 62−63 °C; δ_H (DMSO-d_6) 10.31 (s, 1H, C*H*O), 8.46 (d, 1H, 4.2, −C*H*), 7.89 (d, 1H, 8.7, −C*H*), 7.72 (dd, 1H, 4.3, 8.5, −C*H*), 7.59 (s, 4H, −C*H*), 6.82 (dd, 1H, 17.7, 10.93, −C*H*), 5.94 (d, 1H, 17.7, −CH_2), 5.40 (s, 2H, −OCH_2), 5.36 (d, 1H, 10.93, −CH_2); δ_C (DMSO-d_6) 190.3, 156.5, 141.9, 140.7, 136.8, 136.2, 135.6, 129.23, 127.6, 126.2, 122.6, 114.5, 69.5. ν (KBr pellet): 3071, 2794, 2707, 1706, 1557, 1455, 1290, 1153, 973 cm^{-1}. HRMS, ESI-TOF (+), calcd for $C_{15}H_{14}NO_2$ $(M + H)^+$: 240.1025. Found: 240.1031.

1,3-Bis((*E*)-(3-(4-vinylbenzyloxy)pyridin-2-yl)methyleneamino)propan-2-ol (13). Synthesis followed a procedure developed by Mazurek et al. for preparation of related backbone ligands derived from pyridine-2-carbaldehyde.[18,35] A solution of compound **12** (2.18 g, 9.12 mmol) in 25 mL of methanol was added dropwise to a solution of 1,3-diaminopropan-2-ol (**7**) (0.41 g, 4.6 mmol) in 25 mL of methanol. The resulting solution was stirred overnight and used without further purification for preparation of **8**. A sample aliquot was subjected to analysis by ESI mass spectrometry to verify formation of the title compound. HRMS, ESI-TOF (+), calcd for $C_{33}H_{33}N_4O_3$ $(M + H)^+$: 533.2552. Found: 533.2549.

1,3-Bis((3-(4-vinylbenzyloxy)pyridin-2-yl)methylamino)-propan-2-ol, VB(bpdpo) (8). The volume of the solution of **13** was increased to about 150 mL, and sodium borohydride (0.35 g, 10 mmol) was added in small quantities. After termination of gas evolution, the solution was heated to reflux for 45 min, cooled, and concentrated to dryness. The residue was dissolved in 100 mL of chloroform and extracted once with 15 mL of ice-cold water. The organic layer was separated, dried over anhydrous sodium sulfate, and filtered. The filtrate was concentrated in vacuum, yielding **8** as a yellow-brown oil (2.0 g, 82%). The compound was dissolved in ethanol to produce a 1 M stock solution for subsequent preparation of the Cu(II) complex **1b**.

A sample aliquot of the raw product of **8** was purified on Sephadex LH-20−100 with methanol as eluent; R_f (SiO_2; EtOAc/MeOH, 4/1) = 0.1, yielding **8** as a yellowish oil (65%). This fraction was used for the polymerization experiments. A sample aliquot of this yellowish oil was further purified by preparative-scale HPLC on RP-18 eluting with acetonitrile−water to allow full compound characterization; δ_H ($CDCl_3$) 8.17 (dd, 2H, 4.61, 1.45), 7.42 (dd, 8H, 7.96, 26.53), 7.17 (dd, 2H, 8.34, 1.52), 7.13 (dd, 2H, 8.21, 4.55), 6.74 (dd, 2H, 17.62, 10.93), 5.78 (dd, 2H, 17.56, 0.56), 5.78 (dd, 2H, 17.56, 0.76), 5.29 (dd, 2H, 10.86, 0.76), 5.10 (s, 4H), 4.31 (br s, 1H), 4.05 (s, 4H), 3.83 (s, 1H), 2.81 (dd, 2H, 12.19, 3.73) 2.70 (dd, 2H, 12.19, 8.15); δ_C (DMSO-d_6) 152.0, 149.2, 140.2, 136.8, 136.3, 136.2, 127.8, 126.3, 123.3, 122.6, 119.2, 118.9, 114.5, 79.2, 69.0, 59.9, 53.8, 49.7. IR (thin film on KBr): 3404, 3058, 2918, 1629, 1571, 1443, 1275, 1177, 1116, 992, 910, 829 cm^{-1}. HRMS, ESI-TOF (+), calcd for $C_{33}H_{37}N_4O_3$ $(M + H)^+$: 537.2866. Found: 537.2876.

N,N′*-{Bis((3-(4-vinylbenzyloxy)2-pyridinmethyl)-1,3-diamonopropan-2-ol}ato (μ-acetato) Dicopper Diperchlorate, Cu_2(VBbpdpo) (1b).** A sample aliquot (3.7 mL, 3.7 mmol) of the 1 M ethanol stock solution of **8** was added to a solution of Cu(II) acetate monohydrate (1.6 g, 0.01 mol) in 150 mL of ethanol at ambient temperature. Sodium perchlorate (3.08 g, 0.025 mol) dissolved in 50 mL of ethanol was added, and the resulting solution was stirred for 1 h at ambient temperature. The solution was filtered and concentrated to dryness below 40 °C. Recrystallization of the light blue residue from methanol−dichloromethane yielded complex **1b** as a dark blue amorphous solid (0.83 g, 24%). ***Caution: perchlorate salts are potentially explosive. However, we did not experience any difficulty in handling or drying the compound at or below 40 °C. Anal. Calcd for $C_{35}H_{38}Cl_2Cu_2N_4O_{13}\cdot CH_2Cl_2$: C, 43.00; H, 4.01; N, 5.57. Found: C, 42.86; H, 4.23; N, 5.59. ν_{max} (KBr)/cm^{-1} 3416, 3265, 3092, 2926, 1622, 1577, 1453, 1409, 1352, 1283, 1227, 1092.

■ ASSOCIATED CONTENT

Supporting Information. ^1H and ^{13}C NMR, IR, and ESI mass spectra of all new compounds; cif file for **2b**; stability constants for species derived from **3a**, **8a**, and Cu(II) acetate monohydrate. This material is available free of charge via the Internet at http://pubs.acs.org.

■ AUTHOR INFORMATION

Corresponding Author

*Phone: ++1-334-844-6954. Fax: ++1-334-844-6959. E-mail: Susanne.Striegler@auburn.edu.

■ ACKNOWLEDGMENT

A CAREER award from the National Science Foundation (CHE-0746635) to S.S. is gratefully acknowledged. The authors are also indebted to Thomas E. Albrecht-Schmidt and his research group for analysis of **2b** by X-ray diffraction and to Thomas Webb for insightful comments during the preparation of this manuscript.

■ REFERENCES

(1) Boltje, T. J.; Buskas, T.; Boons, G.-J. *Nat. Chem.* **2009**, *1* (8), 611–622.
(2) Pedersen, C. M.; Schmidt, R. R. *Microb. Glycobiol.* **2009**, 455–476.
(3) Bernardes, G. J. L.; Castagner, B.; Seeberger, P. H. *ACS Chem. Biol.* **2009**, *4* (9), 703–713.
(4) D'Alonzo, D.; Guaragna, A.; Palumbo, G. *Curr. Org. Chem.* **2009**, *13* (1), 71–98.
(5) Dhanawat, M.; Shrivastava, S. K. *Mini-Rev. Med. Chem.* **2009**, *9* (2), 169–185.
(6) Hou, D.; Lowary, T. L. *Carbohydr. Res.* **2009**, *344* (15), 1911–1940.
(7) Huang, L.; Lu, X.; Huang, X. *ACS Symp. Ser.* **2008**, *990* (Chemical Glycobiology), 29–53.
(8) Manabe, S.; Ito, Y. *Curr. Bioact. Compd.* **2008**, *4* (4), 258–281.
(9) Playne, M. J.; Crittenden, R. G. *Nutrafoods* **2008**, *7* (1), 9–18.
(10) Pohl, N. L. *ACS Symp. Ser.* **2008**, *990* (Chemical Glycobiology), 272–287.
(11) Schmidt, R. R.; Vankar, Y. D. *Acc. Chem. Res.* **2008**, *41* (8), 1059–1073.
(12) Smoot, J. T.; Demchenko, A. V. *Adv. Carbohydr. Chem. Biochem.* **2009**, *62*, 161–250.
(13) Stallforth, P.; Lepenies, B.; Adibekian, A.; Seeberger, P. H. *J. Med. Chem.* **2009**, *52* (18), 5561–5577.
(14) Zhu, X.; Schmidt, R. R. *Angew. Chem., Int. Ed. Engl.* **2009**, *48* (11), 1900–1934.
(15) Gichinga, M. G.; Striegler, S. *Chem. Ind.* **2009**, *123* (Catalysis of Organic Reactions), 473–477.
(16) Striegler, S.; Gichinga, M. G. *Chem. Commun.* **2008**, 5930–5932.
(17) Striegler, S. *Tetrahedron* **2006**, *62* (39), 9109–9114.
(18) Striegler, S.; Dittel, M. *J. Am. Chem. Soc.* **2003**, *125* (38), 11518–11524.
(19) Striegler, S.; Dunaway, N. A.; Gichinga, M. G.; Barnett, J. D.; Nelson, A.-G. D. *Inorg. Chem.* **2010**, *49* (6), 2639–2648.
(20) Gichinga, M. G.; Striegler, S.; Dunaway, N. A.; Barnett, J. D. *Polymer* **2010**, *51* (3), 606–615.
(21) Gichinga, M. G.; Striegler, S. *Tetrahedron* **2009**, *65* (25), 4917–4922.
(22) Dittel, M., Ph.D. Thesis, Ulm University, Ulm, Germany, 2003.

(23) Heinert, D.; Martell, A. E. *Tetrahedron* **1958**, *3*, 49–61.
(24) Desideri, N.; Sestili, I.; Manarini, S.; Cerletti, C.; Stein, M. L. *Eur. J. Med. Chem.* **1991**, *26* (4), 455–60.
(25) Attenburrow, J.; Cameron, A. F. B.; Chapman, J. H.; Evans, R. M.; Hems, B. A.; Jansen, A. B. A.; Walker, T. *J. Chem. Soc.* **1952**, 1094–111.
(26) Heimgaertner, G.; Raatz, D.; Reiser, O. *Tetrahedron* **2005**, *61* (3), 643–655.
(27) Farrugia, L. J. *J. Appl. Crystallogr.* **1997**, *30* (5, Pt. 1), 565.
(28) Butcher, R. J.; Diven, G.; Erickson, G.; Jasinski, J.; Mockler, G. M.; Pozdniakov, R. Y.; Sinn, E. *Inorg. Chim. Acta* **1995**, *239* (1−2), 107–16.
(29) X-ray structural analysis: *Cu_2(VBbpdpo)* (**2b**): dark green/blue needle, crystal dimensions 0.300 × 0.070 × 0.066 mm, monoclinic, $P2_1/n$, $Z = 4$, $a = 8.6070(3)$ Å, $b = 20.0239(8)$ Å, $c = 20.9300(8)$ Å, $\beta = 101.4446(8)°$, $V = 3535.5(2)$ Å^3 ($T = 193$ K), $\mu = 14.08$ cm^{-1}, R1 = 0.0440, wR2 = 0.1081. Bruker SMART APEX CCD X-ray diffractometer: $\theta_{max} = 56.58°$, Mo Kα radiation, $\lambda = 0.71073$ Å, 0.3° ω scans, 35 986 reflections measured, 8769 independent reflections all of which were included in the refinement. The data were corrected for Lorentz-polarization effects and absorption (analytical and SADABS); solutions were solved by direct methods; anisotropic refinement of F^2 by full-matrix least-squares, 460 parameters. Further details of the crystal structure investigations may be obtained from the CIF files.
(30) Striegler, S.; Dittel, M. *Inorg. Chem.* **2005**, *44* (8), 2728–2733.
(31) Binstead, R. A.; Jung, B.; Zuberbühler, A. D. *SPECFIT/32 Global Analysis System, 3.0*; Spectrum Software Associates: Marlborough, MA, 2000.
(32) Striegler, S.; Gichinga, M. G.; Dittel, M. *Org. Lett.* **2008**, *10* (2), 241–244.
(33) Gichinga, M. G.; Striegler, S. *J. Am. Chem. Soc.* **2008**, *130* (15), 5150–5156.
(34) Sheehan, J. T. *J. Org. Chem.* **1966**, *31* (2), 636–7.
(35) Mazurek, W.; Bond, A. M.; Murray, K. S.; O'Connor, M. J.; Wedd, A. G. *Inorg. Chem.* **1985**, *24* (16), 2484–90.